RADIO DETECTION OF 18 RASS BL LAC OBJECTS

M. W. B. Anderson[1,2] and M. D. Filipović[2]

[1]*Sydney Observatory, PO Box K346, Haymarket, Sydney, NSW 1238, Australia*
E–mail: *m.filipovic@uws.edu.au*

[2]*University of Western Sydney, Locked Bag 1797*
Penrith South, DC, NSW 1797, Australia

SUMMARY: We present the radio detection of 18 BL Lac objects from our survey of over 575 deg^2 of sky. These 18 objects are located within $20''$ of the X-ray position, of which 11 have a measured red-shift. All candidates are radio emitters above $\sim$1 mJy and fall within the range of existing samples on the two colour, $\alpha_{\rm RO}$ vs $\alpha_{\rm OX}$, diagram with a transitional population of three evident. Two unusual sources have been identified, a candidate radio quiet BL Lac, RX J0140.9–4130, and an extreme HBL, RX J0109.9–4020, with $\log(\nu_{\rm peak}) \approx 19.2$. The BL Lac $\log(N) - \log(S)$ relation is consistent with other samples and indicates the $ROSAT$ All Sky Survey (RASS) could contain (2000 ± 400) BL Lac objects.

Key words. Galaxies: active — BL Lacertae objects: general — quasars: general

1. INTRODUCTION

BL Lac objects are a rare class of active galactic nuclei (AGN, see review by Kollgaard 1994), comprising only $\sim$1.4% of the total AGN population (BL Lac known $\sim$1122, all AGN $\sim$95971, Veron-Cetty and Veron 2006). Standard AGN unification models explain a BL Lac as a near line of sight, non-thermal (i.e. broadband synchrotron emission combined with inverse Compton scattering at higher frequencies), relativistic jet (i.e. Doppler boosting) produced by a FRI radio galaxy nucleus. Consequently, the optical spectrum dominated by continuum emission from the jet is characterised by weak emission or absorption lines. This makes the detection of BL Lacs difficult at optical wavelengths using conventional AGN selection techniques. Most of the existing BL Lac samples have been initially selected at radio or X-ray wavelengths using large area sky surveys, followed by time consuming optical spectroscopy to identify the BL Lacs in the sample. This led to the conclusion that BL Lac characteristics are bimodal, divided into radio selected BL Lacs (RSBL; i.e. the 1 Jy sample of Stickel et al. 1991) and X-ray selected BL Lacs (XSBL, i.e. the *Einstein* Extended Medium Sensitivity Survey (EMSS) sample of Rector et al. 2001).

A model proposed by Giommi and Padovani (1994) unifies BL Lacs as a single population, characterised by a spectral energy distribution (SED) with peak or cutoff of the synchrotron emission in the IR/optical (RSBLs) or in the UV/X-ray (XSBLs). To avoid confusion BL Lac studies use the classification suggested by Padovani and Giommi (1995) of low energy peak BL Lacs (LBLs, mostly RSBL) or high energy peaked BL Lacs (HBLs, mostly XSBL). Both classes exhibit similar extreme "Blazar" activity (see Urry and Padovani 1995) — rapid, irregular variability, high optical polarization, radio core dom-

inated morphology (Laurent-Muehleisen et al. 1993), flat radio spectra, super-luminal motion and emission from the radio to gamma ray bands (Sambruna et al. 1996). Given the EMSS and 1 Jy samples represent extremes of the BL Lac population, Giommi and Padovani (1994) predicted the existence of BL Lacs with properties intermediate to those of LBLs and HBLs — termed intermediate BL Lacs (IBLs).

Currently, our understanding of BL Lac objects is far from complete, due mainly to their rarity limiting the size of statistically complete samples. One area that is poorly understood is the luminosity evolutionary behavior of BL Lacs. While other classes of AGN show a strong trend of positive evolution, BL Lacs do not. LBLs and IBLs exhibit no or a slight positive evolution (Stickel et al. 1991, Rector and Stocke 2001, Laurent-Muehleisen et al. 1999) while HBLs exhibit a negative evolution (Rector et al. 2001), meaning they are less luminous/frequent in the past than now. Although the properties of HBLs and LBLs are different, they are not sufficient to determine if the properties reflect two different populations of AGN's or the extremes of a single continuous AGN population. The role of IBLs remain uncertain (Rector et al. 2003) as their observational properties are not well understood due to the small number known (Laurent-Muehleisen et al. 1999).

In the last 18 years (since the launch of *ROSAT*), the number of BL Lacs has doubled every six to seven years (Fig. 1.) as a direct result of efficient selection techniques (Schachter et al. 1993, Wolter et al. 1997). Stocke et al. (1989) noted that since BL Lacs are radio and X-ray loud, their broadband spectral properties could be used to select out candidate BL Lac objects. In a purely X-ray survey, efficiencies of <5% are reached (Stocke et al. 1991), increasing to ∼10% at $F_X > 10^{-12}$ ergs cm^{-2} s^{-1} (Perlman et al. 1996). In a purely radio survey, ef-

ficiencies of ∼7% are reached (Stickel et al. 1991), increasing to about 12% if flat spectrum sources are pre-selected. In a combined radio and X-ray survey, efficiencies of 10% to 20% or higher can be reached (Schachter et al. 1993, Wolter et al. 1997). Recently, positional correlation of radio and X-ray catalogues has been undertaken: Deep X-ray Radio Blazar Survey (Perlman et al. 1998), the REX Survey (Maccacaro et al. 1998) and the *ROSAT* All Sky Survey – Green bank Survey (RGB; Laurent-Muehleisen et al. 1999). A large sample of 501 radio-selected BL Lac candidates has been compiled by Plotkin et al. (2008) using Faint Images of the Radio Sky at Twenty-Centimetres (FIRST) radio survey in combination with the Sloan Digital Sky Survey (SDSS) optical spectroscopy.

Potentially, the largest complete catalogue of BL Lac objects remains mostly undiscovered in the *ROSAT* All Sky Survey (RASS), a fact first noted by Stocke et al. (1989). Various studies have begun the task of identifying RASS samples of BL Lacs, the RGB sample (127 BL Lacs) of Laurent-Muehleisen et al. (1999) and SDSS/RASS sample of Anderson et al. (2007) with 200 new BL Lacs. The limiting factor for RASS sample sizes is the time consuming task of optical identification with a 15–20″ position error.

Presented in this paper is a sample of 18 new RASS BL Lacs (including five candidate objects and five objects verified from the literature) discovered as part of a radio detection survey and ESO optical identification program for a complete sub-sample of 695 RASS sources. Section 2 describes the RASS sub-sample selection, radio follow-up program and details how optical identifications were made and the criteria used to select objects as BL Lacs. In Section 3 we describe the sample, including a table of BL Lac properties. In Section 4 we examine the properties of the sample and compare them to samples from the literature. Finally, in Section 5 we discuss the findings, with Section 6 forming the conclusion.

2. THE RASS SUB-SAMPLE

The *ROSAT* X-ray telescope completed the first All Sky Survey with an imaging X-ray telescope in 1991, resulting in two RASS Catalogues (unpublished RASS revision one catalogue, ∼54 000 sources, see Voges 1993 and various RASS revision two catalogues, ∼160 000 sources, see Voges 1997 and Voges et al. 1999, 2000). To characterise the source population being detected, a complete sub-sample of four Key Fields, Table 1, was selected (|b| >−25°, δ<10°, 695 sources, covering 575 square degrees) from the revision one catalogue for optical identification (Danziger et al. 1990; European Southern Observatory Key Field Program). To improve the multi-wavelength coverage and to assist the optical program, all Key Field sources where observed at 4.8 GHz (∼1 mJy limit and ∼1″ positional accuracy).
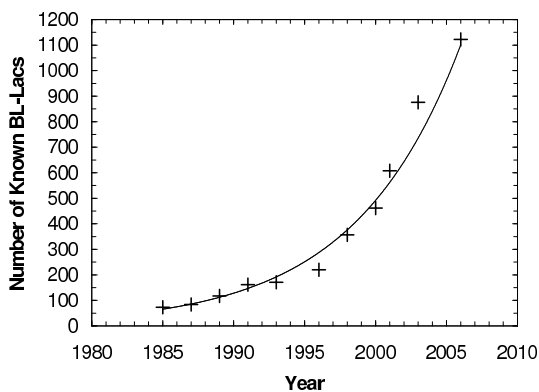

Fig. 1. *Plot of the number of published BL Lac in the literature as a function of time, based on Veron-Cetty and Veron (1984, 1985, 1987, 1989, 1991, 1993, 1996, 1998, 2000, 2001, 2003, 2006). For 2006 ∼1.2% of all known AGNs are BL Lac, compared to ∼88.8% for QSO and ∼10.0% for Sy1. As new ROSAT BL Lacs are discovered the number of known BL Lacs should exceed ∼2000 by 2010.*

Table 1. Summary of the RASS Key Field properties.

Key Field	RA	Dec	Number of Sources
I	01^h	$-40°$	261
II	05^h	$-57°$	227
III	11^h	$-27°$	71
IV	13^h	$+00°$	134

The optical and radio follow-up identified a complete sample of 18 BL Lacs using X-ray positions from the unpublished RASS revision one catalogue. A positional correlation with the RASS revision two catalogue establish all of the objects are real detections.

2.1. Radio follow-up

Radio observations of the BL Lac sample (695) were undertaken as part of the 4.8 GHz radio detection program (Anderson 2003, Anderson et al. 1994). Briefly, the Australia Telescope Compact Array (ATCA) observed the RASS Key Field sources in fields I, II and III, while the Very Large Array (VLA) observed sources in field IV. For the ATCA all observations used a 1.5 km array configurations plus antenna 6 and were made using a 128 MHz bandwidth divided into 32 channels of width 4 MHz. Closest match for the VLA is the C array configuration, with a bandwidth of 50 MHz. All radio detections are located within $2'$ of the pointing centre where bandwidth smearing effects are extremely small. The primary flux calibrators, PKS 1934-638 (ATCA) and 3C286 (VLA), are tied to the VLA absolute flux scale of Baars et al. (1977).

The radio data have been reduced using standard reduction procedures within the Astronomical Image Processing Software (AIPS) package. The observations reached a five sigma detection limit of ~ 2 mJy. All 4.8 GHz flux densities listed in Table 2 have been primary beam corrected.

The radio positions were correlated with the NRAO VLA Sky Survey (NVSS) radio survey (Condon et al. 1998) to determine 1.4 GHz flux densities and errors for BL Lacs north of a declination of $-42°$. Ten coincidences were found, with flux densities listed in Table 2. The efficiency of combined radio (NVSS) and X-ray (RASS) can be as large as 35% (Beckmann et al. 2003). A similar comparison with the Sydney University Molonglo Sky Survey (SUMSS; Mauch et al. 2003) to determine 843 MHz flux densities found four sources, listed in Table 2.

Four BL Lacs were verified by a positional correlation of the Key Field radio positions with BL Lac objects in the NASA/IPAC Extragalactic Database (NED).

2.2. Optical follow-up and identification

Preliminary optical candidates were selected using optical finder charts extracted from the COSMOS catalogue (Yentis et al. 1992). Candidates were prioritised according to distance from the RASS position and optical magnitude, with the priority given to optical sources associated with a radio counter-part. Optical spectroscopy was then used to identify one or more optical candidates until the most likely identification was established.

X-ray selected BL Lacs are X-ray loud and radio loud (Stocke et al. 1991). In practical terms this means all EMSS (Rector et al. 2001) and ESS (Perlman et al. 1996) BL Lacs have a 4.8 GHz flux density brighter than 1 mJy. Hence all RASS BL Lacs should be positionally associated with a radio counterpart brighter than 1 mJy. If all BL Lacs are required to be associated with a radio source then false identification from stellar source with featureless spectrum would also be minimised. In the Key Field sample only one stellar X-ray source (Anderson and Filipović 2007) was detected as a radio emitter.

BL Lac object classification was based on the technique developed for the *Einstein* Extended Medium Sensitivity Survey (Stocke et al. 1991). A source was classified as a BL Lac if it had:

(i) A featureless optical spectrum i.e. no observed emission lines of equivalent width ≥ 0.5 nm.

(ii) A Ca II break of less than 25% to distinguish between a non-thermal AGN spectrum and the stellar spectrum of an elliptical galaxy.

(iii) A 4.8 GHz flux density greater than 1 mJy.

Any candidate BL Lac object was required to meet criterion (iii) and have at least a featureless spectrum.

More details about the optical program are given by Danziger et al. (1990). We recognise that the strength of the Calcium break is depending on the luminosity of the object: the strength of the Calcium break is anti-correlated with the luminosity (Landt et al. 2002, Beckmann et al. 2003). Hence, some BL Lac objects could exhibit Calcium breaks exceeding 25% (Anderson et al. 2007). In addition, blazars can show emission lines. As the BL Lac objects are a subclass of the blazar population and as there is apparently a smooth transition from BL Lacs to Flat Spectrum Radio Quasars (FSRQ), one has to be very careful when applying strict constraints on the optical spectra. While we acknowledge that we might have missed border-line BL Lac objects, the use of criterion (iii) should help reduce the number missed.

3. THE BL LAC SAMPLE

A total of 18 BL Lacs have been identified, their characteristics are summarised in Table 2; Column (1) is the table index for cross referencing with the index in Table 4; Column (2) is the *ROSAT* All Sky Survey Name; Column (3) is the COSMOS J band magnitude; Column (4) is the redshift; Column (5) is the radio position right ascension for J2000; Column (6) is the radio position declination for J2000; Column (7) is the ATCA 4.8 GHz flux density and error in mJy; Column (8) is the 1.4 GHz flux density in mJy from either the Parkes 90 catalogue or the NVSS (only available for sources north of a declination of $-42°$) and associated errors; Column (9) is the reference flag defined at the end of Table 2 and indicates if a source is a candidate or

Table 2. New BL Lacs identified by Key Field program. Table references for column nine: (1) candidate Key Field BL Lac; (2) Confirmed Key Field BL Lac; (3) Confirmed BL Lac from the literature; (4) Schwope et al. (2000); (5) Fischer et al. (1998); (6) Laurent-Muehleisen et al. (1993) and Perlman et al. (1996); (7) Bauer et al. (2000); (8) Cristiani et al. (1995); (9) Xue et al. (2000); (10) Bade et al. (1994); (11) Veron-Cetty and Veron (2006).

(1) Table Index	(2) $ROSAT$ Name	(3) m_J	(4) z	(5) Radio Position (J2000) RA (h m s)	(6) Dec (° ′ ″)	(7) Radio Flux 4.8 GHz (mJy)	(8) 1.4 GHz (mJy)	(9) Ref. Flag	(10) PSPC Count Rate (cts s^{-1})	(11) $N_{\rm H}$ ($\times 10^{20}$ cm^{-2})
1	RX J0040.3–2719	17.6	0.172	00 40 16.4	–27 19 12	53.0±4.7	161.0±4.2	3,7	0.31±0.03	1.51
2	RX J0043.4–2639	17.3	1.00	00 43 22.6	–26 39 07	68.0±5.9	78.0±2.4	3,8	0.04±0.01	1.44
3	RX J0045.8–3158	20.1	0.5	00 45 47.7	–31 58 33	3.4±0.8	4.1±0.6	1	0.06±0.02	1.98
4	RX J0049.7–4151	18.7	0.421	00 49 39.0	–41 51 38	19.3±2.0		1	0.08±0.02	3.19
5	RX J0054.8–2455	17.5		00 54 46.8	–24 55 30	24.5±2.5	24.3±0.9	1	0.18±0.03	1.56
6	RX J0059.5–3510	19.0		00 59 31.5	–35 10 50	39.7±3.7	80.2±2.9	1	0.12±0.02	2.04
7	RX J0109.9–4020‡	19.5	0.313	01 09 56.6	–40 20 51	46.8±4.2	57.4±4.0†	2,4	0.55±0.04	2.66
8	RX J0140.9–4130	17.8		01 40 56.7	–41 30 12	1.9±0.8		2	0.05±0.01	1.79
9	RX J0439.0–5558	18.7		04 39 03.0	–55 58 38	10.7±0.6	†	2	0.17±0.03	1.65
10	RX J0506.9–5435	17.2		05 06 57.8	–54 35 03	15.3±1.3	†	2	0.54±0.06	5.49
11	RX J0528.8–5920	19.2	1.13	05 28 46.1	–59 20 03	19.0±2.0	†	2	0.03±0.01	4.45
12	RX J0543.9–5532	16.7		05 43 57.2	–55 32 08	36.2±2.6	†	2,5	0.69±0.03	7.21
13	RX J1057.8–2753	17.8	0.092	10 57 50.7	–27 54 11	56.0±5.0	63.8±2.0	3,10	0.15±0.02	5.40
14	RX J1103.6–2329	16.2	0.186	11 03 37.6	–23 29 30	58.7±5.2	29.7±1.2	2,6	1.60±0.10	5.64
15	RX J1357.2–0146	16.7	0.546	13 57 13.0	–01 46 01	8.1±1.1	14.9±0.6	1	0.05±0.01	3.48
16	RX J1357.6+0128	16.7	0.219	13 57 38.7	+01 28 14	65.1±5.7	61.3±1.9	2	0.15±0.02	2.36
17	RX J2319.1–4206	15.0	0.055	23 19 05.8	–42 06 49	207.0±17.0†		3,9	0.12±0.03	1.92
18	RX J2324.7–4041	15.5		23 24 44.7	–40 40 49	33.6±3.2		3,11	1.50±0.10	1.79

†RX J2319.1–4206 has a ATCA 4.8 GHz flux density of 207 mJy for the core and 237 mJy for the lob, 444 mJy in total. RX J0109.9–4020 1.4 GHz flux density is for ATESP J010956–402051 from Prandoni et al. (2000). RX J0439.0–5558 has a 843 MHz flux density of 21.2±1.3 mJy for SUMSS J043901–555840 from Mauch et al. (2003), and includes RX J0506.9–5435 with 17.1±1.1 mJy, RX J0528.8–5920 with 18.8±1.0 mJy, RX J0543.9–5532 with 41±2 mJy.

‡For more details see Section 4.1.

confirmed Key Field BL Lac or is from the literature; Column (10) is the RASS count rate and associated error and column (11) is the Total Hydrogen Column Density in units of 10^{20} atoms cm^{-2}. For additional details consult the source notes at the end of this section.

A total hydrogen column density, $N_{\rm H}$, value (Col. 11) is needed to correct the calculated $ROSAT$ Position Sensitive Proportional Counter (PSPC) flux for galactic absorption. Values were estimated for Key Field sources north of a declination of –42° using the Bell Labs H I survey of Stark et al. (1992). For Key Field sources south of a declination of –42°, estimates were taken from the Parkes H I survey of Cleary et al. (1979). Only values from Stark et al. (1992) are not affected by stray radiation entering the far field antenna pattern.

Thirteen (13) BL Lacs, including five candidates, have been optically identified by Danziger et al. (1990) and are listed in Table 2. Up to June 2009, a positional correlation of the radio positions with objects in the NASA/IPAC Extragalactic Database (NED) identified five additional sources classified in the literature as BL Lacs and listed in Table 2.

Multi-epoch 4.8 GHz radio observations, based on a set of 40 sources, indicates the flux density error is well represented by $\sigma_{\rm R} = 0.08 S_{\rm R}^{-1} + 0.48$, with $S_{\rm R}$ the flux density in mJy over the range of 1.5 mJy to 1 Jy. Above 30 mJy the flux error is constant at about 8%, rising to 40% at 1.5 mJy, with errors for individual flux densities given in Table 2.

The number of randomly associated radio counterparts for the entire Key Field sample of 695 RASS objects is estimated at less than two, based on 4.8 GHz radio source counts. This makes the chances of a BL Lac being a random association extremely small.

The Key Field sample is complete to approximately $(9 \pm 2) \times 10^{-13}$ erg cm^{-2} s^{-1}, at which, the prior counts of Wolter et al. (1991) predict a sky density of 0.030±0.008 per degree squared or 17±5 BL Lacs over the 575 deg^2 of sky covered by the four Key Fields. This value compares well to the observed value of 18±4 BL Lacs observed, indicating a high level of completeness. The number of BL Lacs missed is estimated to be less than two.

3.1. Positional accuracy

Astrometric accuracy of the radio and X-ray positions determined by Anderson (2003) are 1.1″ and 30″ respectively. For the radio positions the accuracy was determined by comparing the positions of a standard set of 40 sources observed at two or more epochs, giving a deviation of $\Delta\delta = 0.8''$ and $\Delta\alpha\cos(\delta) = 0.7''$. RASS positional accuracy was de-

termined by comparing the X-ray and radio positions for the ~ 120 radio emitting X-ray sources identified by the Key Field program, with 95% of the radio sources located within 40″ of the X-ray position.

Comparison of the difference between the RASS and ATCA radio positions for the 18 BL Lacs in Fig. 2 indicates 90% of identified sources are located within 15″. This value is smaller than the 30″ error for the entire Key Field sample and is probably due to BL Lac morphology being compact.
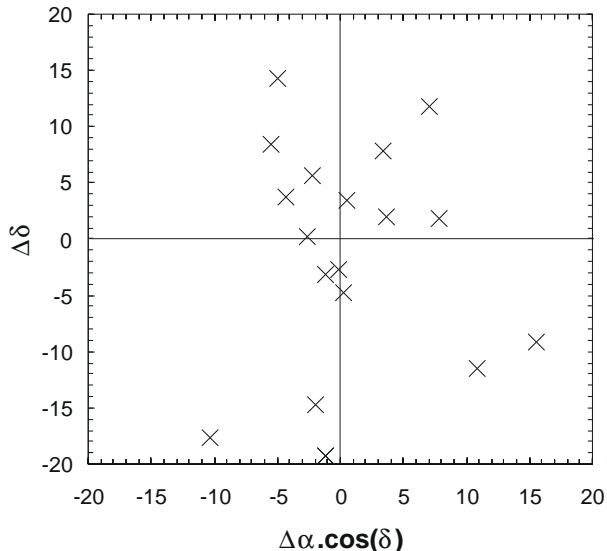
Fig. 2. *The positional difference between the RASS X-ray and the ATCA radio position. All BL Lacs are located within 20″ from the X-ray position.*

3.2. Source notes

BL Lacs classified as candidate objects include the RASS source RX J0049.7–4151, RX J0045.8–3158, RX J0059.5–3510, RX J0054.8–2455 and RX J1357.2–0146.

Objects confirmed as BL Lacs by the ESO optical identification program include RX J0109.9–4020, RX J0140.9–4130, RX J0543.9–5532, RX J0506.9–5435 (also known as 1ES 0505–546), RX J0528.8–5920 (located next to a field galaxy), RX J0528.8–5920, RX J0439.0–5558, RX J1357.6+0128 and RX J1103.6–2329. Multi epoch radio data for RX J0439.0–5558 reveal a variability of 28% or 3 mJy. RX J0109.9–4020 was independently confirmed as a BL Lac (see Schwope et al. 2000), with the radio source PMN J0110–4020 one arcminute away. RX J0543.9–5532 was independently identified in NED as a BL Lac (see Fischer et al. 1998). RX J1103.6–2329 was independently confirmed by Laurent-Muehleisen et al. (1993) and Perlman et al. (1996) as a BL Lac, and is also known as 1ES 1101–232, and PMN J1101–2329 which has

a 4.8 GHz flux density of 66±11 mJy that compares well to the ATCA value.

Five additional objects are classified as BL Lacs in the literature. Bauer et al. (2000) identified RX J0040.3–2719 as a BL Lac and it is also coincident with the radio source NVSS J004016–271912. RX J0043.4–2639 was confirmed as BL Lac by Cristiani et al. (1995), also known as PMN J0043–2639 which has a slightly higher 4.8 GHz flux density of 81±11 mJy compared to the ATCA value 68±6 mJy. Bade et al. (1994) confirmed RX J1057.8–2753 to be a BL Lac object. Veron-Cetty and Veron (2006) confirmed RX J2324.7–4041 (also known as 1ES 2322–409) as a BL Lac.

Xue et al. (2000) investigated RX J2319.1–4206, showing it to be a BL Lac with a complex radio morphology and it is also known as PKS B2316–423 or PMN J2319–4206. The compact core has an ATCA 4.8 GHz flux density of 207 mJy, while the extended lobe has a 237 mJy flux density, giving a total of 444 mJy that compares well to the PMN single dish value of 595 mJy. We also note that this object is very close to the galaxy cluster Abell S1111 located 1.1′ away. This would be indeed very interesting, as BL Lac objects usually seem to avoid cluster environments (Wurtz et al. 1993, 1997). However, upon closer inspection we found that the redshift of RX J2319.1–4206 is z=0.055 and that of Abell S1111 is z=0.045, which gives a difference in distance of $\sim$50 Mpc. Thus, this BL Lac is not likely inside the galaxy cluster.

4. PROPERTIES OF OUR SAMPLE

The characteristics of the sample are examined by comparing it with the *Einstein* EMSS BL Lac sample (Gioia et al. 1990, Rector et al. 2001), the 1 Jy BL Lac sample (Stickel et al. 1991, Rector and Stocke 2001) and the *Einstein* Slew survey (ESS) BL Lac sample (Perlman et al. 1996). The 1 Jy sample is taken to be representative of the properties of Low Energy Peaked BL Lacs (LBLs) and the EMSS of the properties of high energy peaked BL Lacs (HBLs). The ESS exhibits properties that are intermediate between LBLs and HBLs. Comparison was made of the distributions of ν_{peak} (peak frequency of the synchrotron emission), redshift, α_{RO} versus α_{OX}, median spectral index and the X-ray BL Lac $\log(N)$–$\log(S)$. The median values for the four samples are given in Table 3.

Table 3. Median properties of the four BL Lac samples. The median redshift value for this survey is an estimate as only 55% of sources have redshifts.

	EMSS	1 Jy Radio	ESS	This Study
Redshift	0.30	0.55	0.16	0.31
$\log(S_X/S_R)$	–4.8	–6.9	–4.6	–5.0
$\log(\nu_{peak})$	16.2	13.8	15.4	15.9

11

4.1. Peak frequency of the synchrotron emission

The turnover frequency at which the spectral energy distribution (SED) peaks can be used to distinguish LBLs from HBLs. Following Sambruna et al. (1996) and Landau et al. (1986) the key field sample flux densities for the radio (S_R) optical (S_O) and X-ray (S_X) were fitted with a logarithmic parabola of the form:

$$\log(\nu S_\nu) = a(\log(\nu))^2 + b\log(\nu) + c \qquad (1)$$

with ν the observed frequency. The peak frequency is then given by $\log(\nu_{peak}) = -b/2a$ and was k-corrected to the rest frame using $\nu_{rest} = \nu(1+z)$ were ν_{rest} is the rest frame frequency.

For the seven BL Lacs with no measured redshift, a value equal to the sample median (z=0.31, Table 3) is used. While a median will likely underestimate the true redshift (i.e. nearby BL Lacs (z< 0.2) tend to have measured redshift due to the host galaxy being resolved, while objects with no measurable redshift tend to be at z<1) any associated error in α_{RX} due to a k-correction would be smaller then 0.04 for z<1.

Only radio, optical and X-ray data from Table 2 were used. Flux densities were calculated for the PSPC count rate at 2 keV and for the COSMOS optical magnitude at 641 THz using S_O=3.95×10^{-23} $10^{-0.4m(J)}$ adopted from Fukugita et al. (1995) for S_O values calculated within the NED database. An example of the SED and functional fit for one source is given in Fig. 3. The k-corrected peak values are listed in Table 4. A fit to source 7 (RX J0109.9–4020) was problematic, giving a very high peak frequency that has been placed in parentheses in Table 4. Examination of the broad band fluxes shows the X-ray count rate is abnormally high (see Sect. 5).

Fig. 4 compares the two point radio to X-ray spectral index, α_{RX}, versus $\log(\nu_{peak})$ diagram for this sample (Table 4) with that of the one Jy Radio and the EMSS using values from the literature (Sambruna et al. 1996). Clearly α_{RX} and $\log(\nu_{peak})$ are correlated. A linear regression analysis of the Key Field data, excluding one anomalous point (source 7 marked with ‡ in Table 2 and plotted as solid diamond in Fig. 4), results in:

$$\alpha_{RX} = -0.091 \times \log(\nu_{peak}) + 2.12,$$

in good agreement to the fit of Dong et al. (2002),

$$\alpha_{RX} = -0.09535 \times \log(\nu_{peak}) + 2.16065,$$

based on the EMSS and 1 Jy radio samples.

Two lines defined by α_{RX}=0.75 and $\log(\nu_{peak})$=14.7 in Fig. 4. can be used to delineate four regions. HBLs occupy the lower right quadrant and LBLs the upper left quadrant. This distinction was first suggested by Dong et al. (2002) and is equivalent to using $\log(S_R/S_X)$=–5.5 (Laurent-Muehleisen et al. 1999) as a criterion. Intermediate BL Lacs occupy the region defined by α_{RX}=0.7 to α_{RX}=0.8.

The Key Field sample is composed mostly of 13 HBLs, three IBLs and two others falling within the region for LBLs. A median $\log(\nu_{peak})$=15.9 (Table 3) is close to the EMSS value of 16.2, both are typical of HBLs. As expected, the ESS with IBLs has a median value $\log(\nu_{peak})$=15.4 that falls close to halfway between the LBLs (1 Jy sample) $\log(\nu_{peak})$=13.8 and the HBLs $\log(\nu_{peak})$=16.2 (EMSS).

Table 4. Values of the spectral indices for radio to optical, optical to X−ray and radio to X−ray, the logarithm of the frequency for the SED turnover peak and the type of BL Lac, LBL, IBL and HBL. Note that Col. 1 (Index) is for cross referencing with Table 1.

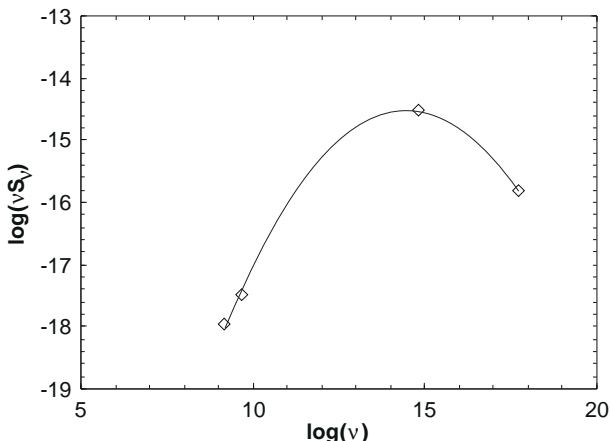| Index	α_{RO}	α_{OX}	α_{RX}	$\log(\nu_{peak})$	Type
1	0.42	1.12	0.70	15.9	HBL
2	0.41	1.52	0.83	14.8	LBL
3	0.38	0.99	0.63	16.6	HBL
4	0.42	1.09	0.69	16.0	HBL
5	0.35	1.22	0.68	15.5	HBL
6	0.50	1.03	0.72	16.4	IBL
7	0.56	0.66	0.64	(19.2)	HBL
8	0.15	1.37	0.60	15.3	HBL
9	0.37	1.03	0.64	16.3	HBL
10	0.28	0.94	0.55	16.8	HBL
11	0.46	1.17	0.74	15.8	IBL
12	0.32	0.94	0.57	16.8	HBL
13	0.44	1.07	0.69	16.0	HBL
14	0.32	0.90	0.56	16.9	HBL
15	0.36	1.14	0.67	15.9	HBL
16	0.37	1.33	0.73	15.2	IBL
17	0.33	1.66	0.82	14.4	LBL
18	0.22	1.17	0.58	15.8	HBL

Fig. 3. *Example of the logarithmic parabola (Eq. 1) fitted to the spectral energy distribution of source RX J0043.4–2639, Table 4, with the observed $log(\nu_{peak})$=14.81.*
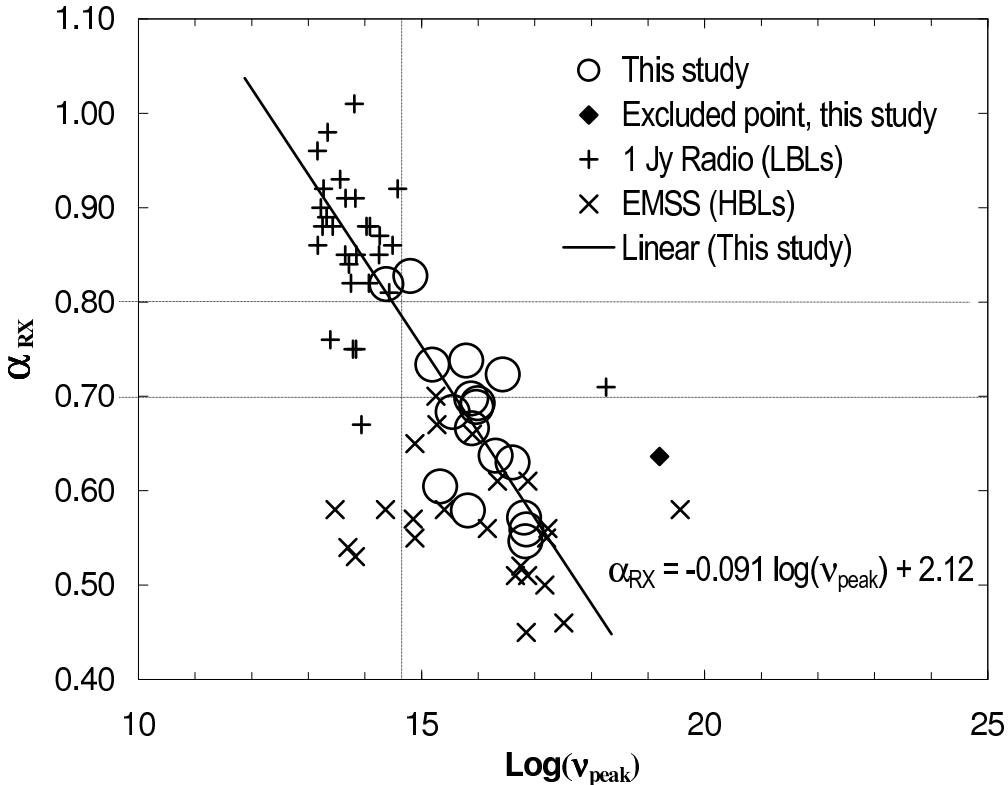
Fig. 4. *The positional difference between the RASS X-ray position and the ATCA radio position. All BL Lacs are located within 20″ from the X-ray position.*

4.2. Redshift distribution

The Key Field sample has 11 BL Lacs with measured redshifts (eight have z<0.5, three have z>0.5) and seven with no redshift. Six of the seven with no redshift are bright (i.e. m_J<18) and have $\log(S_{m(J)}/S_X)$ typical of objects in the EMSS with z<0.8 (Stocke et al. 1991). The median redshift of the sample (z=0.31) is consistent with the EMSS (z=0.30) and is placed about halfway between median value for the ESS (z=0.16) and 1 Jy (z=0.55) samples. Similarly, the median z and $\log(S_X/S_R)$ for the three samples and the Key Field value of $\log(S_X/S_R)$=−5.0 corresponds to an interpolated median z of 0.35±0.4.

The Key Field sample indicates a sample of HBLs has a systematically lower redshifts than a LBLs (i.e. 1 Jy) sample. This finding is consistent with the unification model of Fossati et al. (1997), which predicts HBLs to have systematically lower redshifts compared to LBLs, meaning that HBLs have lower intrinsic luminosities than LBLs. A slight correlation was found for the Key Field and EMSS sample between z and $\log(\nu_{peak})$, indicating $\log(\nu_{peak})$ increases with z. The same variables do not correlate for the 1 Jy sample.

4.3. Spectral index

The method of Brinkmann and Siebert (1994) was used to estimate a spectral index for each BL Lac using hardness ratios. The hardness ratios for each BL Lac have large errors that make the estimated spectral index values uncertain. Therefore, only the sample median value will be presented. For the 18 sources the median energy index is 1.42±0.80 and compares well with the values from the literature, 1.32±0.40 for a RASS sample (Laurent-Muehleisen et al. 1999) and 1.47±0.40 for the EMSS (Rector et al. 2001).

4.4. α_{RO} versus α_{OX} diagram

Fig. 5 is the α_{RO} versus α_{OX} plot for the Key Field and comparison samples. The two point spectral index is calculated using α_{RO}=$\log(S_R/S_O)/\log(\nu_R/\nu_O)$ and α_{OX}=$\log(S_O/S_X)/\log(\nu_O/\nu_X)$ with flux densities evaluated at ν_R=4.8 GHz, ν_O=641 THz (COSMOS III-aJ Photographic B magnitude is ∼ B λ=4400 Å, see Sect. 4.1 for further details) and ν_X = 5.40×10^{17} Hz (X-ray flux density is calculated for 2 keV). The flux densities have been k-corrected to the rest frame
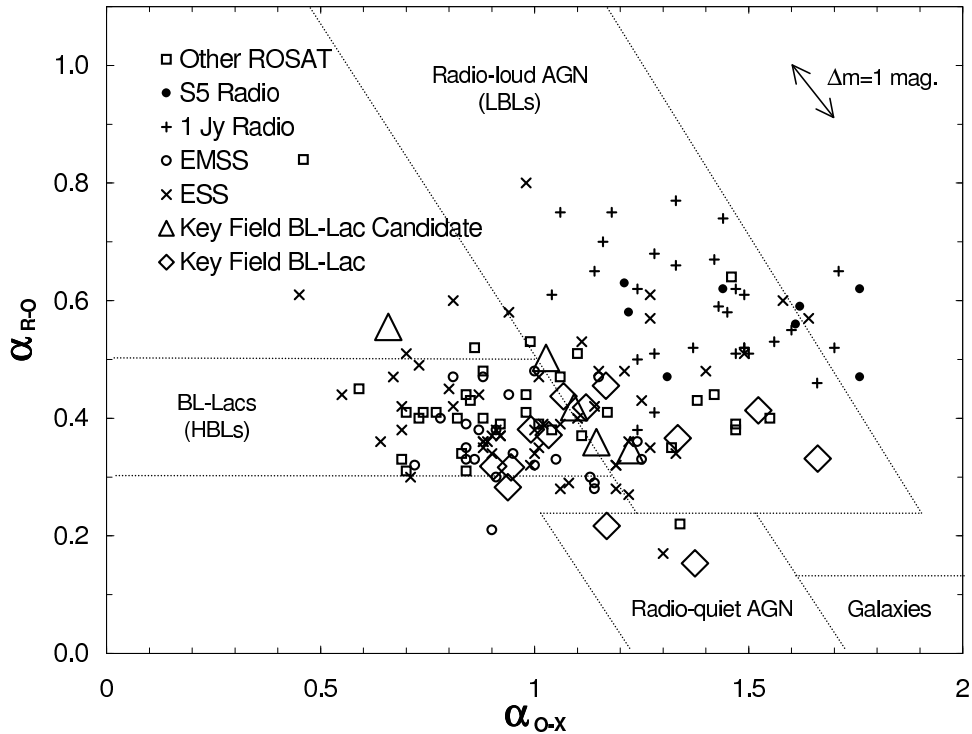
13

Fig. 5. *Radio to optical versus optical to X-ray spectral index plot for BL Lac objects. The Key Field sample, including candidate objects, are plotted as a large diamond and triangle, respectively. Other samples shown are for comparison and are drawn from X-ray selected samples; Einstein EMSS (Giommi et al. 1995), Einstein Slew survey (ESS; Perlman et al. 1996), other ROSAT BL Lacs and radio selected BL Lacs; 1 Jy and S5 (Stickel et al. 1991). The regions defining different types of objects, and the definition of α_{RO} and α_{OX}, are taken from the Einstein EMSS (Stocke et al. 1991). A one magnitude optical variation is shown in the top right corner.*

(i.e. $S_{rest}=S\times(1+z)^{\alpha-1}$), assuming α_R=0.0, α_O=1.0 and α_X=1.2), with the median sample redshift (Table 3) used if none are available. The final values are listed in Table 4, along with α_{RX}. Comparison values are based on data in the literature.

The one anomalous ν_{peak} value from Sect. 4.1 corresponds to an extreme outlier in the α_{RO} versus α_{OX} plane above the main BL Lac region. The value is flagged in Table 4 by brackets and is likely unrepresentative of the overall distribution (see Sect. 5).

The other 15-points (4 candidate and 11 confirmed), likely HBLs, are positioned within the regions occupied by the EMSS and the 1 Jy samples. Two points, likely IBLs, are located in the radio quiet region, but are still within the region occupied by ESS BL Lacs.

4.5. X−ray log (N) − log (S)

The X-ray source counts (Fig. 6) are consistent with the EMSS and the ESS counts. They have a slight bump at f_X=10^{-11} erg cm^{-2} s^{-1} reported by Maccacaro et al. (1989) and Nass et al. (1996). The EMSS counts fall well below the Key Field

level as does the ESS count. This is partially due to incompleteness of the EMSS to bright X-ray sources and the ESS to faint X-ray sources between $\sim2\times10^{-12}$ erg cm^{-2} s^{-1} and 10^{-11} erg cm^{-2} s^{-1}.
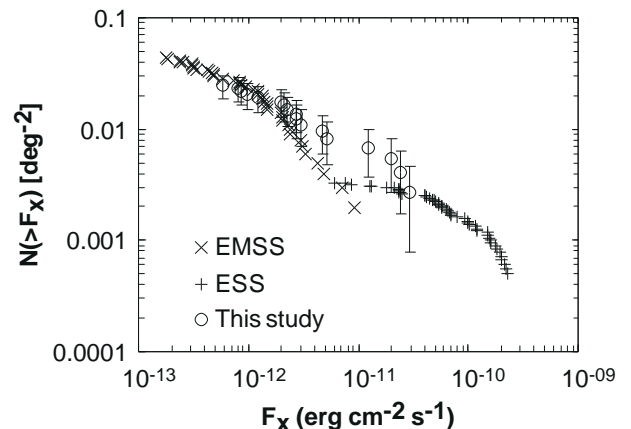

Fig. 6. *X-ray log (N)-log (S) for the Key Field BL Lacs and comparison samples. All error bars are based on the count error.*

If one takes the flux limit of the RASS as $\sim 3 \times 10^{-13}$ erg cm^{-2} s^{-1} (0.1-2.4 keV) that would correspond to a sky density of 0.04 BL Lacs per square degree. At this density, the RASS will contain $(2.6 \pm 0.4) \times 10^3$ BL Lacs for the whole sky, reducing to $(2.0 \pm 0.4) \times 10^3$ at high galactic latitudes. At this density the RASS will contain $(2.6 \pm 0.4) \times 10^3$ BL Lacs for the whole sky, reducing to $(2.0 \pm 0.4) \times 10^3$ at high galactic latitudes.

5. DISCUSSION

A candidate radio quiet BL Lac, RX J0140.9–4130, with a 1.8 mJy flux density occupies the radio quiet AGN region of the α_{RO}–α_{OX} plot at α_{RO}=0.15 (Fig. 5). A total of 16 BL lacs in the sample have $\alpha_{RO} > 0.3$, more than double the 0.15 value. This contrasts to most X-ray selected samples that tend to be X-ray loud and radio loud (Stocke et al. 1991).

The unusual source, RX J0109.9–4020, has a SED with a very high synchrotron peak frequency with $\log(\nu_{peak}) \approx 19.2$. Using all available flux measurements we looked for possible abnormal flux values that might explain the high $\log(\nu_{peak})$ value. No indication of variability was found, while using only fluxes close to the X-ray flux epoch (1991) does not alter the $\log(\nu_{peak})$ value. The only noticeable difference is that the RASS flux is significantly high relative to the other optical and X-ray fluxes i.e. $\alpha_{RO} = 0.66$ while $\alpha_{OX} > 1$ for the 17 other objects. Alternatively, RX J0109.9–4020 could be an example of a new population of BL Lacs, possibly a ultra high energy peaked BL lac predicted by Ghisellini (1999) to have a peak frequency ν_{peak} located at higher frequencies than HBLs, $\log(\nu_{peak}) > 18$. Nieppola et al. (2006) and Wu et al. (2009) showed for a large BL Lac sample there is a population of extreme HBL with $\log(\nu_{peak})$ values extending out to 21.5.

Traditionally, the α_{RO}–α_{OX} plot has been used to demonstrate the divisions of the population. These boundaries have proven successful in identifying new BL Lac objects, achieving efficiencies of $\sim 20\%$ (e.g. *Einstein* Slew Survey (ESS); Perlman et al. 1996, Schachter et al. 1993). If the EMSS colour-colour boundaries had been strictly applied to the Key Field BL Lacs then up to seven BL Lacs would have been missed.

A problem facing BL Lac samples is the use of selection criteria and the associated biases introduced. An example of this is the observed bimodality between LBLs (1 Jy) and HBLs (Key Field and EMSS) which is partly due to BL Lac selection, in that the 1 Jy and EMSS/Key-field samples contain objects biased to the selection of BL Lacs using radio or X-ray properties only. Laurent-Muehleisen et al. (1999) showed the *ROSAT* Green bank BL Lac sample has no bimodality owing to a large number of intermediate BL Lacs.

By cutting off the Key Field sample to simulate an X-ray and Radio selected sample should reproduce the observed bimodality. The EMSS limit in the *ROSAT* band is about 3×10^{-2} μJy (Laurent-Muehleisen et al. 1999), giving a median $\log(S_X/S_R)$=–4.8, which is exactly the same as the EMSS (HBL) value, Table 3. The only bright radio source in the sample was taken to be representative of the 1 Jy sample, giving $\log(S_X/S_R)$= –6.7 for the total flux, which is the same as the 1 Jy (LBL) median value of –6.9. Clearly even the Key Field sample can reproduce the observed bimodality between HBL and LBL.

6. CONCLUSION

The primary result of this paper is the sample of 18 BL Lacs presented in Table 2. Based on the sample properties (Table 4), there are two LBL, three IBLs and 13 HBLs, making HBLs over represented, compared to LBLs that make up only 11% of objects, as expected for a primarily X-ray selected sample. By applying appropriate X-ray and radio flux limits to the sample we were able to reproduce the observed bimodality between LBLs (1 Jy) and HBLs (EMSS). Two unusual sources have been identified, a candidate radio quiet BL Lac, RX J0140.9–4130, and an extreme HBL, RX J0109.9–4020, with a very high synchrotron peak frequency $\log(\nu_{peak}) \approx 19.2$. A slight positive correlation was found between ν_{peak} and redshift.

A correlation between α_{RX} and $\log(\nu_{peak})$ was also found, defined by the fit $\alpha_{RX} = -0.091 \log(\nu_{peak}) + 2.12$, and it is in good agreement with the fit of Dong et al. (2002). The fit can be used to directly calculate ν_{peak} when no optical flux is available.

Two main problems are faced by BL Lac studies, understanding the SED and how it relates to the properties of the underlying source population, and the small number of known objects. A number of major programs are constructing large BL Lac samples (≈ 500) by combining the RASS (Anderson et al. 2007) or FIRST (Plotkin et al. 2008) surveys with the SDSS for identification. At a flux limit of $\sim 3 \times 10^{-13}$ erg cm^{-2} s^{-1} (0.1–2.4 keV), the RASS contains ~ 2592 BL Lacs for the whole sky, reducing to ~ 2000 at high galactic latitudes. Even a complete sample of only 500 objects would allow major progress to be made in understanding the BL Lac phenomena. Our concept of existing BL Lac objects based on radio or X-ray selection may need to be modified to fit into potentially new BL Lac populations suggested by optical selections of Londish et al. (2002) and Collinge et al. (2005).

tem: we have also used data obtained from the High Energy Astrophysics Science Archive Research Center (HEASARC), which is provided by NASA's Goddard Space Flight Center. We thank the referee for his/her excellent comments that have greatly improved this manuscript.

REFERENCES

Anderson, M. W. B.: 2003, A Radio Survey Of Selected Fields From The ROSAT All Sky Survey, Ph. D. Thesis, University of Western Sydney.

Anderson, M. W. B., Filipović, M. D.: 2007, *Mon. Not. R. Astron. Soc.*, **381**, 1027.

Anderson, M. W. B., White, G. L., Ekers, R. D., Danziger, J.: 1994, The First Stromlo Symposium: The Physics of Active Galaxies. ASP Conference Series, **54**, 355.

Anderson, S. F., Margon, B., Voges, W., et al.: 2007, *Astron. J.*, **133**, 313.

Bade, N., Fink, H. H., Engels, D.: 1994, *Astron. Astrophys.*, **286**, 381.

Baars, J. W. M., Genzel, R., Pauliny-Toth, I. I. K., Witzel, A.: 1977, *Astron. Astrophys.*, **61**, 99.

Bauer, F. E., Condon, J. J., Thuan, T. X., Broderick, J. J.: 2000, *Astrophys. J. Suppl. Series*, **129**, 547.

Beckmann, V., Engels, D., Bade, N., Wucknitz, O.: 2003, *Astron. Astrophys.*, **401**, 927.

Brinkmann, W., Siebert, J.: 1994, *Astron. Astrophys.*, **285**, 812.

Cleary, M. N., Haslam, C. G. T., Heiles, C.: 1979, *Astron. Astrophys. Suppl. Series*, **36**, 95.

Condon, J. J., Cotton, W. D., Greisen, E. W., Yin, Q. F., Perley, R. A., Taylor, G. B., Broderick, J. J.: 1998, *Astron. J.*, **115**, 1693.

Collinge, M. J., Strauss, M. A., Hall, P. B., et al.: 2005, *Astron. J.*, **129**, 2542.

Cristiani, S., La Franca, F., Andreani, P., et al.: 1995, *Astron. Astrophys. Suppl. Series.*, **112**, 347.

Danziger, I. J., Trümper, J., Beuermann, K., et al.: 1990, *ESO Messenger*, **62**, 4.

Dong, Y-M., Mei, D-C., Liang, E-W.: 2002, *Publ. Astron. Soc. Japan*, **54**, 171.

Fischer, J.-U., Hasinger, G., Schwope, A. D., Brunner, H., Boller, T., Trümper, J., Voges, W., Neizvestny, S.: 1998, *Astron. Nachr.*, **319**, 347.

Fossati, G., Celotti, A., Ghisellini, G., Maraschi, L.: 1997, *Mon. Not. R. Astron. Soc.*, **289**, 136.

Fukugita, M., Shimasaku, K., Ichikawa, T.: 1995, *Publ. Astron. Soc. Pacific*, **107**, 945.

Ghisellini, G.: 1999, *Astrophysical Letters and Communication*, **39**, 17.

Gioia, I. M., Maccacaro, T., Schild, R. E., Wolter, A., Stocke, J. T., Morris, S. L., Henry, J. P.: 1990, *Astrophys. J. Suppl. Series*, **72**, 567.

Giommi, P., Ansari, S. G., Micol, A.: 1995, *Astron. Astrophys. Suppl. Series*, **109**, 267.

Giommi P., Padovani P.: 1994, *Mon. Not. R. Astron. Soc.*, **268**, L51.

Kollgaard, R. I.: 1994, *Vistas in Astronomy*, **38**, 29.

Landau, R., Golisch, B., Jones, T. W., et al.: 1986, *Astrophys. J.*, **308**, 78.

Landt, H., Padovani, P., Giommi, P.: 2002, *Mon.*

Not. R. Astron. Soc., **336**, 945.

Laurent-Muehleisen, S. A., Kollgaard, R. I., Moellenbrock, G. A., Feigelson, E. D.: 1993, *Astron. J.*, **106**, 875.

Laurent-Muehleisen, S. A., Kollgaard, R. I., Feigelson, E. D., Brinkmann, W., Siebert, J.: 1999, *Astrophys. J.*, **525**, 127.

Londish, D., Croom, S. M., Boyle, B. J., et al.: 2002, *Mon. Not. R. Astron. Soc.*, **334**, 941.

Maccacaro, T., Gioia, I. M., Schild, R. E., Wolter, A., Morris, S. L., Stocke, J. T.: 1989, BL Lac Objects, Ed:, L. Maraschi, T. Maccacaro, M.-H. Ulrich, Springer-Verlag, 222.

Maccacaro, T., Caccianiga, A., della Ceca, A., Wolter, A., Gioia, I. M.: 1998, *Astron. Nachr.*, **319**, 15.

Mauch, T., Murphy, T., Buttery, H. J., Curran, J., Hunstead, R. W., Piestrzynski, B., Robertson, J. G., Sadler, E. M.: 2003, *Mon. Not. R. Astron. Soc.*, **342**, 1117.

Nass, P., Bade, N., Kollgaard, R. I., Laurent-Muehleisen, S. A., Reimers, D., Voges, W.: 1996, *Astron. Astrophys.*, **309**, 419.

Nieppola, E., Tornikoski, M., Valtaoja, E.: 2006, *Astron. Astrophys.*, **445**, 441.

Padovani, P., Giommi, P.: 1995, *Astrophys. J.*, **444**, 567.

Perlman, E. S., Stocke, J. T., Schachter, J. F., et al.: 1996, *Astrophys. J. Suppl. Series*, **104**, 251.

Perlman, E. S., Padovani, P., Giommi, P., Sambruna, R., Jones, L. R., Tzioumis, A., Reynolds, J.: 1998, *Astron. J.*, **115**, 1253.

Plotkin, R. M, Anderson, S. F., Patrick B. Hall, P. B., Margon, B., Voges, W., Schneider, D. P., Stinson, G., York, D. G.: 2008, *Astron. J.*, **135**, 2453.

Prandoni, I., Gregorini, L., Parma, P., de Ruiter, H. R., Vettolani, G., Wieringa, M. H., Ekers, R. D.: 2000, *Astron. Astrophys. Suppl. Series*, **146**, 41.

Rector, T. A., Stocke, J. T.: 2001, *Astron. J.*, **122**, 565.

Rector, T. A., Stocke, J. T., Perlman, E. S., Morris, S. L., Gioia, I. M.: 2001, *Astron. J.*, **120**, 1626.

Rector, T. A., Gabuzda, D. C., Stocke, J. T.: 2003, *Astron. J.*, **125**, 1060.

Sambruna, R. M., Maraschi, L., Urry, C. M.: 1996, *Astrophys. J.*, **463**, 444.

Schachter, J. F., Stocke, J. T., Perlman, E., et al.: 1993, *Astrophys. J.*, **412**, 541.

Schwope, A., Hasinger, G., Lehmann, I., et al.: 2000, *Astron. Nachr.*, **321**, 1.

Stark, A. A., Gammie, C. F., Wilson, R. W., Bally, J., Linke, R. A., Heiles, C., Hurwitz, M.: 1992, *Astrophys. J. Suppl. Series*, **79**, 77.

Stickel, M., Fried, J. W., Kuehr, H., Padovani, P., Urry, C. M.: 1991, *Astrophys. J.*, **374**, 431.

Stocke, J. T., Morris, S. L., Gioia, I. M., Maccacaro, T., Schild, R. E., Wolter, A.: 1989, BL Lac Objects: Proceedings of a workshop held in Como, Italy, September 20-23, 1988, Springer-Verlag, 242.

Stocke, J. T., Morris, S. L., Gioia, I. M., Maccacaro, T., Schild, R., Wolter, A., Fleming, T. A., Henry, J. P.: 1991, *Astrophys. J. Suppl. Series*, **76**, 813.

Urry, C. M., Padovani, P.: 1995, *Publ. Astron. Soc. Pacific*, **107**, 803.

Veron-Cetty, M. P., Veron, P.: A catalogue of quasars and active nuclei (1th Edition), 1984, ESO, 1.

Veron-Cetty, M. P., Veron, P.: A catalogue of quasars and active nuclei (2nd Edition), 1985, ESO, 1.

Veron-Cetty, M. P., Veron, P.: A catalogue of quasars and active nuclei (3rd Edition), 1987, ESO, 1.

Veron-Cetty, M. P., Veron, P.: A catalogue of quasars and active nuclei (4th Edition), 1989, ESO, 1.

Veron-Cetty, M. P., Veron, P.: A catalogue of quasars and active nuclei (5th Edition), 1991, ESO, 1.

Veron-Cetty, M. P., Veron, P.: A catalogue of quasars and active nuclei (6th Edition), 1993, *ESO Sci. Rep.*, **13**, 1.

Veron-Cetty, M. P., Veron, P.: A catalogue of quasars and active nuclei (7th Edition), 1996, *ESO Sci. Rep.*, **17**, 1.

Veron-Cetty, M. P., Veron, P.: A catalogue of quasars and active nuclei (8th Edition), 1998, *ESO Sci. Rep.*, **18**, 1.

Veron-Cetty, M. P., Veron, P.: A catalogue of quasars and active nuclei (9th Edition), 2000, *ESO Sci. Rep.*, **19**, 1.

Veron-Cetty, M. P., Veron, P.: A catalogue of quasars and active nuclei (10th Edition), 2001, *ESO Sci. Rep.*, **20**, 1.

Veron-Cetty, M. P., Veron, P.: 2003, *Astron. Astrophys.*, **412**, 399.

Veron-Cetty, M. P., Veron, P.: 2006, *Astron. Astrophys.*, **455**, 773.

Voges, W.: 1993, *Adv. Space Res.*, **13**, 391.

Voges W.: 1997, Proc. 5th workshop Data Analysis in Astronomy, Eds. V. Di Gesu, M. J. B., Duff, A. Heck, M. C. Maccarone, L. Scarsi, H. U. Zimmermann, World Sci. Pub. Co., 189.

Voges, W., Aschenbach, B., Boller, Th., Bruninger, H., et al.: 1999, *Astron. Astrophys.*, **349**, 389.

Voges, W., Aschenbach, B., Boller, Th., Bruninger, H., et al.: 2000, *IAUC*, **7432**, 1.

Wolter A., Gioia, I. M., Maccacaro, T., Morris, S. L., Stocke, J. T.: 1991, *Astrophys. J.*, **369**, 314.

Wolter A., Ciliegi P., Della Ceca R., Gioia I. M., Giommi P., Henry J. P., Maccacaro T., Padovani P., Ruscica C.: 1997, *Mon. Not. R. Astron. Soc.*, **284**, 225.

Wu, Z., Gu, M., Jiang, D. R.: 2009, *Research in Astronomy & Astrophysics*, **9**, 168.

Wurtz, R., Ellingson, E., Stocke, J. T., Yee, H. K. C.: 1993, *Astron. J.*, **106**, 869.

Wurtz, R., Ellingson, E., Stocke, J. T., Yee, H. K. C.: 1997, *Astrophys. J.*, **480**, 547.

Xue, S., Zhang, Y., Chen, J.: 2000, *Astrophys. J.*, **538**, 121.

Yentis D. J., Cruddace R. G., Gursky H.: 1992, Proceedings of the Conference on Digitised Optical Sky Surveys, Editors, H. T. MacGillivray, E. B. Thomson, Kluwer Academic Publishers, Dordrecht, Boston, MA, 67.

РАДИО ДЕТЕКЦИЈА 18 RASS BL LAC ОБЈЕКАТА

M. W. B. Anderson[1,2] and M. D. Filipović[2]

[1]*Sydney Observatory, PO Box K346, Haymarket, Sydney, NSW 1238, Australia*

E–mail: *m.filipovic@uws.edu.au*

[2]*University of Western Sydney, Locked Bag 1797 Penrith South, DC, NSW 1797, Australia*

У овој студији представљамо радио-детекцију 18 нових BL Lac објеката са нашег прегледа неба од преко 575 квадратних степени. Ових 18 објеката се налазе на мање од 20″ од положаја у X подручју. За 11 од 18 објеката имамо измерени црвени помак. Свих 18 кандидата су радио-емитери изнад ~1 mJy и потпадају у познату групацију од "две боје", α_{RO} vs α_{OX}, дијаграм са евидентном транзиционом популацијом 3. Детектовали смо и два веома необична извора: кандидат за радио-тиху BL Lac, RX J0140.9–4130, и екстремни HBL, RX J0109.9–4020, са $\log(\nu_{peak}) \approx 19.2$. BL Lac $\log(N)$–$\log(S)$ релација је конзистентна са осталим узорцима и указује да *ROSAT* All Sky Survey (RASS) има и до (2000 ± 400) BL Lac објеката.